Dependence of bending losses on cladding thickness in plastic optical fibers

Gaizka Durana, Joseba Zubia, Jon Arrue, Gotzon Aldabaldetreku, and Javier Mateo

Our main goal is to provide a comprehensive explanation of the existing differences in bending losses arising from having step-index multimode plastic optical fibers with different cladding thicknesses and under different types of conditions, namely, the variable bend radius R, the number of fiber turns, or the fiber diameter. For this purpose, both experimental and numerical results of bending losses are presented for different cladding thicknesses and conditions. For the measurements, two cladding thicknesses have been considered: one finite and another infinite. A fiber in air has a finite cladding thickness, and rays are reflected at the cladding-air interface, whereas a fiber covered by oil is equivalent to having an infinite cladding, since the very similar refractive index of oil prevents reflections from occurring at the cladding-oil interface. For the sake of comparison, numerical simulations based on ray tracing have been performed for finite-cladding step-index multimode waveguides. The numerical results reinforce the experimental data, and both the experimental measurements and the computational simulations turn out to be very useful to explain the behavior of refracting and tunneling rays along bent multimode waveguides and along finite-cladding fibers.

OCIS codes: 060.0060, 060.2270, 060.2300, 060.2310.

1. Introduction

Plastic optical fibers (POFs) constitute a relatively mature type of optical fibers. Their attenuation has been their main drawback for a long time, to the extent of reducing researchers' interest. However, since the recent improvement achieved in their attenuation,[1–4] POFs have been objects of intense study. This improvement has come mainly from their having reduced extrinsic losses, namely, absorption of fiber pollutants (transition metals and organic compounds), scattering originated by dust particles, microfractures and bubbles, and radiation losses coming from perturbations in the fiber geometry. Present manufacturing techniques have made this reduction possible and, in the near future, further improvements are expected, in both intrinsic and extrinsic losses.[5]

Optical power losses derived from bends in optical fibers are of considerable importance, especially in telecommunications systems, since they diminish the link optical margin.[6,7] All rays in a bent fiber are leaky; at successive reflections they lose power by either refraction or tunneling.[8–14]

It is common, especially in theoretical treatments, for one to consider optical fibers with an infinite cladding thickness; this means that rays refracted at the core-cladding interface are lost forever. However, in real fibers the cladding itself acts as a waveguide, allowing refracted rays to return back to the core after being guided in the cladding. This effect may lead to a wrong estimation of bending losses and to a bad measurement of some important fiber parameters, such as numerical aperture and bandwidth.

To avoid these effects, it is a quite common practice to use cladding mode strippers.[15] These exist in a fiber section from which the coating has been removed. Then the bare fiber is immersed in a fluid of refractive index that is very close to that of the cladding to reduce reflections occurring at the cladding-fluid interface as much as possible. In this way rays will escape from the fiber, and the cladding will behave as if it were infinite.

In this paper we present experimental and computational results that underline the importance of fiber cladding thickness in power losses in bent step-index multimode fibers. Results have been particularized for POFs. The numerical results from the computer

G. Durana, J. Zubia, J. Arrue, and G. Aldabaldetreku are with the Escuela Superior de Ingenieros de Bilbao, Universidad del Pais Vasco, Alameda Urquijo S/N, Bilbao 48013, Spain. J. Mateo is with the Centro Politécnico Superior, Universidad de Zaragoza, Zaragoza 50015, Spain.

Received 3 April 2002; revised manuscript received 8 October 2002.

0003-6935/03/060997-06$15.00/0

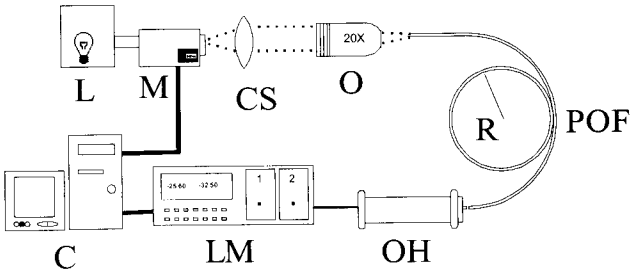

Fig. 1. Diagram showing the experimental setup. L, white light source; M, monochromator; CS, convergent lens; O, object lens; POF, plastic optical fiber; R, cylinder with radius R; OH, optical head; LM, lightwave multimeter; C, computer.

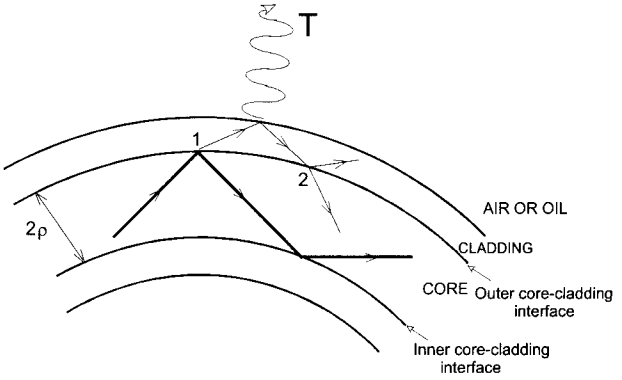

Fig. 2. Typical ray path in a bent fiber of finite cladding thickness. The classical path in the core is shown with a thick line. The other ray paths represent guided rays as a consequence of the finite cladding thickness.

simulations, which are intended to complement the information provided by the experimental results, show the same behavior as those from the experiments. This analysis can indicate which rays participate more actively in bending losses.

The structure of the paper is as follows. First, we present the experimental method and the model used to simulate bends in POFs. Next, experimental results as well as simulation results are exposed. Finally, we discuss these results and present the main conclusions we have reached.

2. Experiment

An experimental setup was mounted to obtain the output power from a bent fiber put in oil or in air, as shown in Fig. 1. The wavelength was selected by means of a halogen lamp followed by a monochromator. The monochromator included a stepper motor, controlled by the computer, in order to select the light wavelength automatically.

The convergent lens serves to collimate the divergent beam coming from the monochromator into an object lens that couples the beam into the fiber, exciting in this way all the modes at the fiber input (the numerical aperture of the object lens is greater than that of the POF). Then the bare fiber is wound several full turns, from one to ten, onto poly(methyl methacrylate)(PMMA) cylinders of different radii. In some measurements the wound POF is immersed in oil (n_{oil} = 1.47) to simulate an infinite cladding, while in others the cylinder is put in air (finite-cladding thickness). In all of the cases the entrance of the bent is placed just after the fiber input, where the launching conditions are kept constant, in order to have the same input conditions at the entrance of the fiber bent section.

Most of the measurements were carried out with the 1-mm-diameter bare fiber Super Eska SK-40 and the rest with bare fibers of 0.75 and 0.5 mm (Super Eska SK-30 and SK-20, respectively). The core and cladding refractive indices were n_{co} = 1.492 and n_{cl} = 1.402, respectively, for all of the POFs.[16] In the experiments, five PMMA cylinders were used for bending the POF, with radii ranging from 5.1 to 20.0 mm, although the most representative measurements correspond to the three smallest ones (cylinder radii: 5.1, 7.6, and 10.25 mm). The results were averaged for three POF samples. The overall fiber length (2 m) and launching conditions were kept constant in all the experiments.

3. Ray-Tracing Model

Apart from the laboratory measurements, a numerical analysis has been developed with MATLAB. The computer program simulates a step-index multimode waveguide of length L, which is wound onto a cylinder of radius R. The software calculates the power arriving at the end of the bent waveguide when the cladding thickness is both finite and infinite. The calculus takes into account only meridional rays in order to reduce the computational time. The simulation controls the power conveyed by each type of ray (refracting rays and tunneling rays), which seems to be very useful to understand the light propagation inside the bent fiber.

When a finite-cladding thickness is considered (air covered), the simulation software calculates not only ray paths inside the waveguide core but also rays traveling into the cladding. Because these rays can be guided in the cladding owing to refractive-index differences between cladding (n_{cl} = 1.402) and air (n = 1), they are able to return back to the core and continue their path in it. Therefore they must be taken under control, as they are of great importance in the final energy balance.

However, a finite-cladding thickness adds great complexity to the software program, and some approximations have to be made. First of all, we have to notice that each time a refracting ray finds the core-cladding interface, two rays are created. This is illustrated in Fig. 2. In this case, the ray is refracting at the outer core-cladding interface and tunneling at the inner core-cladding interface. The classical core ray path, when the cladding is assumed infinite, is marked with a thick curve. Other ray paths drawn in the figure represent guided rays as a consequence of the finite-cladding thickness. At those core-cladding interface points where the ray is refracting (1 and 2 in the figure) two rays appear from

the incident ray, one reflected and another refracted, and both with a considerable power content. This means that, after several fiber turns, the number of rays derived from one initial launched ray will be enormous, more than 2^N. Including them in the simulation is a complex task. Nevertheless, most of these rays will convey a negligible amount of energy, and they can be excluded from both the simulation and the final energy balance. The approximations used will be discussed later on.

In the simulation, parallel rays making an angle θ_z ($\theta_z < \theta_c$) with the fiber axis (inside the fiber) at the beginning of the bent section are considered. Then, depending on the rays that are refracting or tunneling, different power transmission coefficients are used. For refracting rays, the classical Fresnel coefficient applies (scalar approximation):

$$T_r = \frac{4 \sin \theta_i (\sin^2 \theta_i - \sin^2 \theta_c)^{1/2}}{[\sin \theta_i + (\sin^2 \theta_i - \sin^2 \theta_c)^{1/2}]^2}, \quad (1)$$

where θ_i is the angle of incidence that the ray makes with the tangent to the core-cladding interface and θ_c is the complementary critical angle $\theta_c = \cos^{-1}(n_{cl}/n_{co})$.

For tunneling rays the power transmission coefficient is

$$T_t = \frac{4 \sin \theta_i}{\sin \theta_c} \left(1 - \frac{\sin^2 \theta_i}{\sin^2 \theta_c}\right)^{1/2} \exp[-2/3 n_{co} k \times (R + \rho)(\theta_c^2 - \theta_i^2)^{3/2}], \quad (2)$$

where n_{co} is the core refractive index, $k = 2\pi/\lambda$, R is the bending radius, and ρ is the waveguide core radius. For typical values of the parameters ($n_{co} = 1.492$, $n_{cl} = 1.402$, $\theta_c = 20.0°$, $\rho = 0.49$ mm, $R = 10$ mm, and $\lambda = 650$ nm), T_t is very small ($T_t \approx 10^{-8}$). Therefore we have considered $T_t = 0$, which means that tunneling rays do not lose power throughout the bent waveguide, except for a few very close to the critical angle.

As stated above, each refracting ray generates a lot of new refracting rays, their number depending on the waveguide length, although only a few of them have been considered in the numerical analysis, namely, those that convey the most energy. As the majority of refracting rays have transmission coefficients at the core-cladding interface greater than $T_r = 0.5$, the criterion to select rays was as follows: Each time a ray had a transmission coefficient higher than 0.5 at the core-cladding interface, we chose the transmissive way to continue. Of course, when oil is surrounding the fiber, the transmitted part of these rays into the cladding is not guided, and they are forever lost.

4. Results

A. Experimental Results

In Fig. 3 we show the power in decibels detected at the fiber output relative to the unbent POF fiber (P_{rel}) as a function of the wavelength for a 1-mm-diameter POF and a bend radius of $R = 5.1$ mm. Different curves correspond to different numbers of full turns around the cylinder. It can be seen from the curves that the received power is quite independent of the light wavelength. The small wavelength dependence of the received power can be attributed to tunneling rays and to the core refractive-index dependence with wavelength, $n_{co} \equiv n_{co}(\lambda)$.

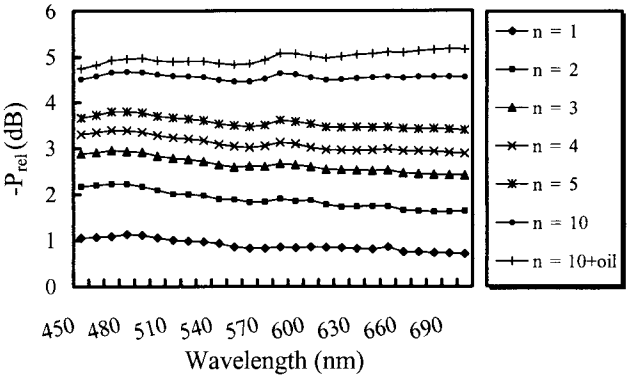

Fig. 3. Output power in decibels relative to the unbent POF as a function of wavelength for a different number of full turns around the cylinder of radius $R = 5.1$ mm. Fiber diameter considered: $d_{POF} = 1$ mm.

Figure 4 summarizes the experimental results obtained for a 1-mm-diameter bare POF and $\lambda = 540$ nm. In this plot, the relative output power as a function of the number of full turns is represented for different bend radii. We observe two features: first, the gradual stabilization of bending losses as we increase the number of turns, and second, the sharp increase in losses as we reduce the cylinder diameter. The increase is particularly important for the smallest cylinder radius, namely, $R_1 = 5.1$ mm. In addition, data corresponding to ten fiber turns dipped in oil is also included. A comparison between data corresponding to ten full turns in air and in oil shows that the received power is smaller in the case of oil environment. This suggests that more rays escape from the POF and thus that the infinite-cladding condition is quite reasonable when we have matching oil covering the POF.

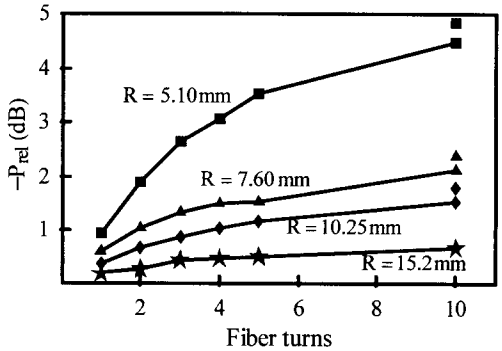

Fig. 4. Measured relative output power as a function of the number of full turns. Different curves correspond to different bend radii. The case of ten fiber turns dipped in oil is also included.

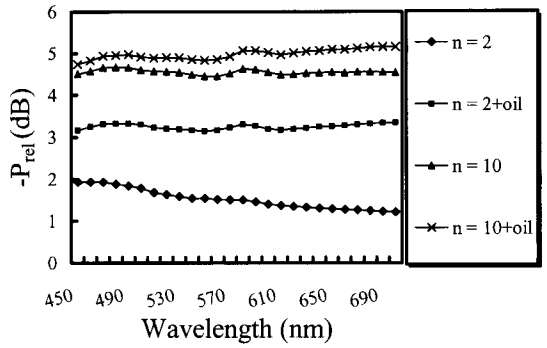

Fig. 5. Detected relative output power as a function of the wavelength for $n = 2$ and $n = 10$ fiber turns, with and without oil.

The power detected at the POF output as a function of the wavelength for $n = 2$ and $n = 10$ fiber turns, with and without oil, is represented in Fig. 5. The important thing here is to realize that the gap existing between the curves corresponding to oil and air environments is bigger for a small number of turns.

Figure 6 shows, for a fixed value of the wavelength ($\lambda = 540$ nm), the power gap $P_1 - P_2$, in decibels, between the oil-covered and the air-covered bent POFs for different bend radii R and for two different numbers of turns ($n = 2$ and $n = 10$). P_1 is the output power for the POF immersed in oil, and P_2 is the output power when the entire POF is surrounded by air. As we increase the bend radius, curves corresponding to different conditions go to zero ($P_1 - P_2 \approx 0$ for $R \geq 15$ mm), indicating that no guided rays are in the cladding. It is also interesting to note that the curve for the $n = 2$ fiber turns is always above that for $n = 10$.

Figure 7 shows the experimental values of the power difference $P_2 - P_1$ for different values of the bend radius R and different POF core diameters. The number of fiber turns considered was $n = 2$. Note that, for a fixed value of the bend radius R, the difference becomes more important as the core diameter increases. This is because, for a fixed bend radius R, the curvature of the outer core-cladding interface is smaller for bigger values of the fiber core diameter, and thus less refracting rays are generated.

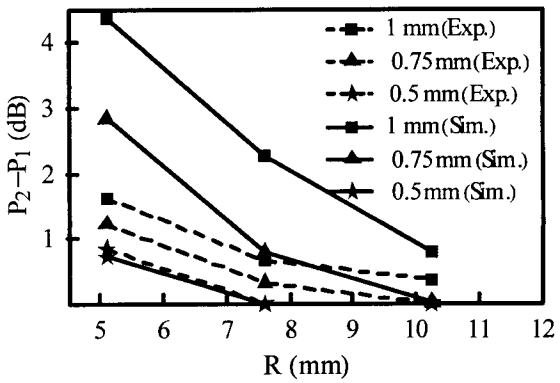

Fig. 7. Power difference $P_2 - P_1$ at the POF exit for different bending radii and $n = 2$ fiber full turns. Experimental as well as computational results are presented for three fiber diameters: $d_1 = 1.00$, $d_2 = 0.75$, and $d_3 = 0.50$ mm.

B. Simulation Results

In Figs. 6 and 7, both the experimental results and the numerical values obtained from the computer simulations have been plotted. In both graphs, experimental and simulation values follow the same behavior, although they cannot be directly compared, because the launching conditions are different in both cases. Results from simulations tend to give more losses because only meridional rays have been taken into account, which are the most lossy ones. In the experimental case only a few rays are meridional, so the overall result is that the attenuation of rays is smaller.

Figure 8 shows how the cladding thickness modifies the output power of the air-covered fiber. In this simulation, we have considered a bend radius R of 8 mm and two fiber turns ($n = 2$). The output power varies with cladding thickness, the results approach-

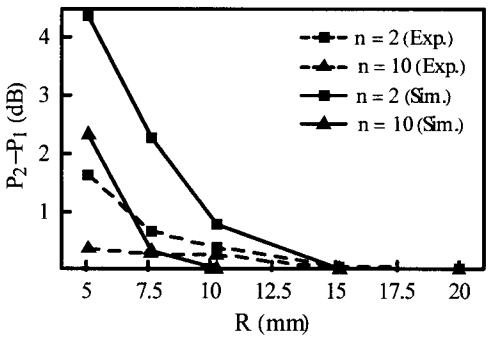

Fig. 6. Representation of the power difference $P_2 - P_1$ at the fiber output for different bend radii R and for $n = 2$ and $n = 10$ fiber turns. P_1, power received when the bent section of the fiber is dipped in oil; P_2, power received when the entire fiber is left in air. Experimental as well as computational results are presented for a fixed value of the wavelength ($\lambda = 540$ nm).

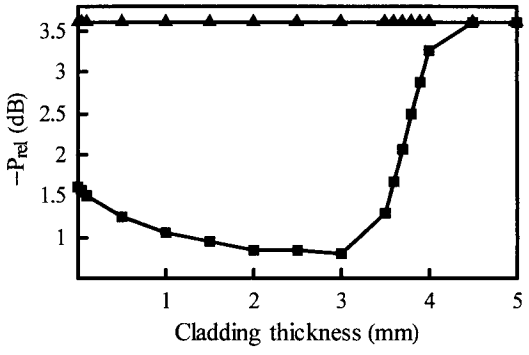

Fig. 8. Simulated values of the relative output power for different cladding thicknesses when the fiber is covered by air (squares) and by oil (triangles). As the cladding thickness increases, the curve corresponding to the air-covered POF converges to the straight line that corresponds to the fiber dipped in oil (congruent to the infinite cladding thickness).

ing those in oil environment as cladding thickness is increased (straight curve, independent of cladding thickness). Nevertheless, the output power first increases with cladding thickness until a maximum of power is reached, and then it decreases asymptotically to the straight line. The origin of this initial power increase with cladding thickness may be explained easily. As the cladding thickness is increased, for a certain fiber length, refracted rays have fewer collisions, and thus fewer transmission coefficients have to be considered. In addition to this, all of these rays are tunneling at the cladding-air interface, and almost all of their power is reflected back to the cladding. After reaching a maximum, output power starts to decrease. This happens because rays start to be refractive at the cladding-air interface (they are no longer tunneling), and a lot of power is transmitted to the air. This transmission of power to the air is stronger than the power gained by the fiber as a consequence of reducing the number of collisions, and the overall energy balance is negative. From this figure we deduce that we need several millimeters for the cladding to be considered as infinite, which is unpractical from a manufacturing point of view. This means that calculations based on infinite-cladding thickness give always greater losses than the real ones; in our case more than 1 dB greater.

5. Discussion

When bending losses are considered there are several factors to be taken into account: fiber core diameter, bend radius, bent section length or fiber turns, and fiber environment. There are some other factors, such as numerical aperture, refractive-index profile, or launching conditions, that also have influence on bending losses of POFs but that have been kept constant in our experiments. Their treatment will be presented elsewhere.

In the previous section we saw that decreasing the bend radius, as well as increasing the fiber core diameter, increases the bending losses. Therefore it is recommendable, if we want to reduce losses, to use optical fibers with the smallest possible fiber core diameter that is compatible with the system we want to design, and to bend the fibers with the greatest radius possible. We observe in Fig. 4 that for bend radii greater than or equal to $R = 15$ mm and $n = 1$ (1 fiber turn), the losses are practically zero, and that for a greater number of fiber turns the losses increase, but still remain very low. Also, for $R = 15$ mm, no difference is observed between results with and without oil, indicating that there are no refracting rays at all. As the bend radius begins to decrease, more and more refracting rays are produced and more power is transferred to the cladding. Matching the cladding with oil causes most of the refracting rays in the cladding to go out, making it impossible for them to return to the core. For this reason, output power decreases. Fortunately, in practice, small-bend radii are quite infrequent in optical fiber systems and installations.

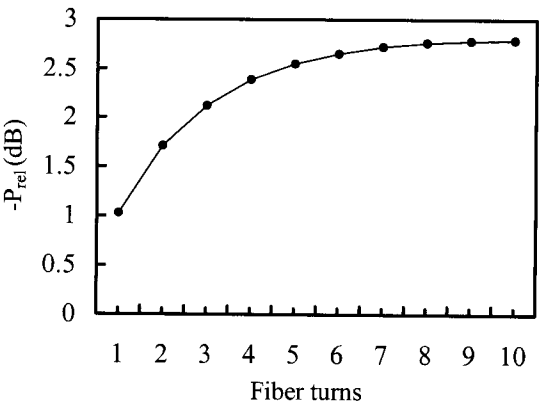

Fig. 9. Numerical simulation showing the power received at the waveguide output as a function of the number of waveguide turns around a cylinder of radius $R = 8.00$ mm. The waveguide is covered by air. Waveguide core diameter, 980 μm; cladding thickness, 10 μm; $n_{core} = 1.492$; $n_{cladding} = 1.402$.

The loss also increases with the length of the bent fiber, although the greatest increase occurs with the second fiber turn. However, the increment in loss when going from n to $n + 1$ fiber turns, n being 2 or greater, is smaller. This fact is clearly shown in Fig. 4 for a bend radius of 5.1 mm and also in the numerical simulation shown in Fig. 9 for a bend radius of 8.0 mm, core radius $\rho = 0.49$ mm, and cladding thickness $1 = 10$ μm. We can explain these results in terms of rays, considering the behavior of tunneling and refracting rays inside the bent fiber. Refracting rays have greater transmission coefficients compared with those of tunneling rays [see Eqs. (1) and (2) for transmission coefficients]. The initial rapid loss of power is due to rays incident at the core-cladding interface with angles θ_i that are greater than the critical angle θ_c, which yield high values in the transmission coefficient. These are refracting rays, and they lose a great part of their energy at the beginning of the bent fiber. Once the refracting rays have lost most of their energy, the rate of loss is slower, and the remaining losses are due mainly to weakly leaky rays (tunneling rays or whispery gallery rays).

The aspect that has been studied more carefully in this paper is the dependence of the surrounding medium on bending losses. Air and oil have been used in our study. As we have pointed out, oil matches the refractive index of the cladding, which is equivalent to an infinite cladding. This approach serves to compare real data with that coming from theoretical treatments, which are developed on the assumption that the cladding is infinite. According to the experimental results and the numerical simulations, the power detected at the output end of the fiber in air (P_1) and oil (P_2) environments differs from each other only when the bend radius is small. For big enough bending radii ($R = 15$ mm or greater in our measurements) there is no difference ($P_1 - P_2 \cong 0$), but, when small enough bend radii are taken into account, the difference is quite important, especially with one or two fiber turns (see Figs. 5 and 6). In fact, when the

bend radius decreases, maintaining the rest of the parameters as fixed, the number of rays refracted from the core to the cladding increases. We will assume that all these rays are guided in the cladding when air is surrounding the fiber (a reasonable supposition if we consider that the critical angle at the cladding-air interface is quite big, $\theta_c \approx 45°$, and that the cladding thickness very small, $1 \cong 10$ μm). Then the difference $P_1 - P_2$ is just the power conveyed by these refracted rays that are guided in the cladding. This shows quite clearly the reason of such a dependence of $P_1 - P_2$ on the bend radius. The fact that the difference $P_1 - P_2$ is more important for $n = 2$ than for $n = 10$ fiber turns (see Fig. 5) can be explained by recalling that the rays refracted to the cladding convey more energy at short distances from the start of the bent fiber than at longer ones (at these distances refracted rays are energetically weakened). Thus for $n = 2$ turns the amount of energy that is conveyed to the cladding and guided $(P_1 - P_2)$ is greater than that for $n = 10$ fiber turns.

6. Conclusions

This paper shows, both experimentally and numerically, the influence of the finite-cladding thickness on bending losses in step-index multimode plastic optical fibers. Specifically, it clearly shows that, for big enough bend radii ($R \geq 15$ mm), no difference in bending losses is appreciated between the finite and the infinite cladding fibers. However, when finite-cladding thicknesses and smaller bend radii are considered, bending losses are partly covered up by ray guidance in the cladding. For the same results in both cases (finite and infinite cladding), a cladding that is several millimeters thick would be needed, which is far away from being realistic. The oil covering the bent section of the fiber turns out to be a good fluid for the experimental determination of the bending losses that are theoretically estimated under the infinite-cladding thickness assumption. The differences in bending losses owing to the aforementioned factors will be of special interest if the power budget is an important factor to be controlled in our system.

We thank the Universidad del País Vasco-Euskal Herriko Unibertsitatea and the Ministerio de Ciencia y Tecnología, under projects 1/UPV/EHU00147.345-TA-8035/200 and TIC2000-059, for their financial support.

References

1. Y. Koike, T. Ishigure, and E. Nihei, "High-bandwidth graded index polymer optical fiber," J. Lightwave Technol. **13,** 1475–1489 (1995).
2. Y. Koike, "Progress in GI-POF_Status of high speed plastic optical fiber and its future prospect," in *Proceedings of the Ninth International Conference on Plastic Optical Fibres and Applications–POF'00, Boston, Massachusetts, 2000* (Information Gatekeepers, Boston, Mass., 2000), pp. 1–5.
3. T. Ishigure, E. Nihei, and Y. Koike, "Optimum refractive index profile for graded-index polymer optical fibres, toward gigabit data links," Appl. Opt. **35,** 2048–2053 (1996).
4. M. Naritomi, "Model home project in Japan using GI-POF," in *Proceedings of the Ninth International Conference on Plastic Optical Fibres and Applications–POF'00, Boston, Massachusetts, 2000* (Information Gatekeepers, Boston, Mass., 2000), pp. 8–11.
5. M. Naritomi, "CYTOP Amorphous Fluoropolymers for low loss POF," in *POF Asia Pacific Forum 1996, Tokyo, Japan, 1996* (POF Consortium, Tokyo, Japan, 1996), p. 23.
6. A. W. Snyder and J. D. Love, *Optical Waveguide Theory* (Chapman and Hall, London, 1983).
7. D. S. Jones, *The Theory of Electromagnetism* (Pergamon, New York, 1964).
8. C. Winkler, J. D. Love, and A. K. Ghatak, "Loss calculations in bent multimode optical waveguides," Opt. Quantum Electron. **11,** 173–183 (1979).
9. A. Ghatak, E. Sharma, and J. Kompella, "Exact paths in bent waveguides," Appl. Opt. **27,** 3180–3184 (1988).
10. A. W. Snyder and D. J. Mitchell, "Generalized Fresnel's laws for determining radiation loss from optical waveguides and curved dielectric structures," Optik (Stuttgart) **40,** 438–459 (1974).
11. J. D. Love and C. Winkler, "Power attenuation in bent multimode step-index slab and fiber waveguides," Electron. Lett. **14,** 32–34 (1978).
12. C. Winkler, J. D. Love, and A. K. Ghatak, "Power attenuation in bent parabolic-index slab and fiber waveguides," Electron. Lett. **14,** 570–571 (1978).
13. A. W. Snyder and J. D. Love, "Reflection at a curved dielectric interface-electromagnetic tunnelling," IEEE Trans. Microwave Theory Tech. **MTT-23,** 134–141 (1975).
14. D. Gloge, "Bending loss in multimode fibers with graded and ungraded core index," Appl. Opt. **11,** 2506–2513 (1972).
15. A. P. Boechat, D. Su, D. R. Hall, and D. C. Jones, "Bend loss in large multimode optical fiber beam delivery system," Appl. Opt. **30,** 321–327 (1991).
16. "High performance plastic fiber optics, ESKA™," technical leaflet, Mitsubishi Rayon Co., Tokyo, Japan.